Title: Male-biased recombination at chromosome ends in a songbird revealed by precisely mapping crossover positions

Running title: Male-biased recombination in a songbird

All (co-)authors:

Hongkai Zhang[*,1], hongkai.zhang@biol.lu.se, ORCID ID: 0000-0001-7371-9612

Max Lundberg[1], max.lundberg@biol.lu.se, ORCID ID: 0000-0002-1895-3622

Suvi Ponnikas[2], suvi.ponnikas@gmail.com, ORCID ID: 0000-0003-3526-2118

Dennis Hasselquist[1], dennis.hasselquist@biol.lu.se, ORCID ID: 0000-0002-0056-6616

Bengt Hansson[*,1], bengt.hansson@biol.lu.se, ORCID ID: 0000-0001-6694-8169

[1]Department of Biology, Lund University, 22362 Lund, Sweden

[2]Department of Biology, University of Oulu, 90570 Oulu, Finland

[*]Corresponding authors

Keywords: Recombination; Crossover; Male bias; Sub-telomeric regions; SNP; Songbird; Great reed warbler

Abstract: Recombination plays a crucial role in evolution by generating novel haplotypes and disrupting linkage between genes, thereby enhancing the efficiency of selection. Here, we analyse the genomes of twelve great reed warblers (*Acrocephalus arundinaceus*) in a three-generation pedigree to identify precise crossover positions along the chromosomes. We located more than 200 crossovers and found that these were highly concentrated towards the telomeric ends of the chromosomes. While the number of recombination events was similar between the sexes, the crossovers were located significantly closer to the ends of paternal compared to maternal chromosomes. The frequency of crossovers was similar between intergenic and genic regions, but within genes, they occurred more frequently in exons than in introns. In conclusion, our study of the great reed warbler revealed substantial variation in crossover frequencies within chromosomes, with a distinct bias towards the sub-telomeric regions, particularly on the paternal side. These findings emphasise the importance of thoroughly screening the entire length of chromosomes to characterise the recombination landscape and uncover potential sex-biases in recombination.

Article summary: The genetic exchange between the paternal and maternal chromosomes during meiosis – recombination – plays a crucial role in evolution by generating new haplotypes that natural selection can act upon. By analysing genomic data of a three-generation family of great reed warblers, we detected precise locations of approximately 200 recombination events in the genome of these birds. This unveiled a prominent sex-bias with recombination occurring more often towards chromosome ends in males than in females.

1 Introduction

Recombination has profound evolutionary implications by generating new haplotypes that natural selection can act upon. The process of reshuffling haplotypes through recombination breaks linkage disequilibrium and reduces the interference between linked loci, which

otherwise limits the action of natural selection (Felsenstein 1974; Otto 2021). Recombination disconnects beneficial and deleterious alleles at linked loci, facilitating adaptive evolution (increasing the frequency of advantageous alleles) and purging the genetic load (reducing the frequency of deleterious alleles). The Y and W chromosomes of mammals and birds illustrate the importance of recombination, as their prolonged periods without recombination have resulted in significant degeneration and paucity of genes (Charlesworth and Charlesworth 2000; Bachtrog 2013).

Recombination not only has evolutionary implications but can also be subject to selection and undergo evolutionary changes itself. Studies have demonstrated variation in recombination rates across clades, species, populations, and between sexes (Ritz et al. 2017; Stapley et al. 2017; Peñalba and Wolf 2020). For example, fungi generally exhibit higher rates of recombination (averaging 48.7 cM/Mb) compared to plants (averaging 1.9 cM/Mb) (Stapley et al. 2017), and among mammals, recombination rates range from 0.2 cM/Mb in opossums to 1.6 cM/Mb in dogs (Dumont and Payseur 2008). The variation in recombination rate across species and deeper lineages can be attributed, at least in part, to evolved differences in chromosome size and number. The presence of more and smaller chromosomes tends to increase recombination rates since each chromosome (or chromosome arm) requires a minimum of one crossover (CO) on one of the two sister chromatids (Coop and Przeworski 2007; Stapley et al. 2017). Regarding sex differences, the most extreme scenario is when recombination is entirely absent in one sex (achiasmy). This lack of recombination coincides almost exclusively with the heterogametic sex, such as male *Drosophila* (XY) and female Lepidoptera (ZW) (Haldane 1922; Huxley 1928; John et al. 2016). However, in many plants and animals, the degree of sexual dimorphism in recombination (heterochiasmy) is less pronounced, with at least some level of recombination in both sexes (Burt et al. 1991; Broman et al. 1998; Maddox et al. 2001; Berset-Brändli et al. 2008; Wellenreuther et al.

2013; Bergero et al. 2019; Malinovskaya et al. 2020). Generally, it is not surprising that recombination can evolve since it exhibits typical features of evolving traits, such as variation among individuals and a heritable component, as seen in humans (Kong et al. 2004) and sheep (Johnston et al. 2016). In fact, evidence from experimental populations in *Drosophila* shows that the rate of recombination can be manipulated over short evolutionary time scales (Aggarwal et al. 2015; Kohl and Singh 2018).

Quantifying the recombination landscape – the local recombination rate variation along the chromosomes – can provide valuable insights into the influence of recombination on various biological processes. For instance, as selection operates on chromosome regions (linked selection), low recombining regions often exhibit reduced selection efficiency at single mutations, lower local effective population size (N_e), and stronger genetic drift (Peñalba and Wolf 2020). Moreover, recombination can contribute to elevated GC content through GC-biased gene conversion (Mugal et al. 2015) and increase genetic variation by locally raising the mutation rate (Filatov and Gerrard 2003; Hellmann et al. 2003; Huang et al. 2005; Arbeithuber et al. 2015; Halldorsson et al. 2019). As expected, the local recombination rate correlates with various population genetic parameters, including linkage disequilibrium, nucleotide diversity, GC and repeat content, and gene density (Peñalba and Wolf 2020; Ponnikas et al. 2022). A common pattern observed in many species is an increase in recombination rates towards the telomeres and decreasing rates around the centromeres (Vincenten et al. 2015; Limborg et al. 2016; Haenel et al. 2018; Sardell and Kirkpatrick 2020). Mechanistically, heterochromatin, which is enriched around the centromeres, can prevent local recombination by hindering polymerase accessibility or through repression of double-strand break (DSB) formation caused by methylation, RNAi or specific enzymes (Ellermeier et al. 2010; Melamed-Bessudo and Levy 2012; Wijnker et al. 2013). Quantifying the recombination landscape allows the identication of recombination hotspots where

recombination is particularly frequent, as well as cold spots, where recombination is infrequent. Notably, detailed analysis of recombination hotspots in humans and mice led to the discovery of the *PRDM9* gene as a key regulator of the local recombination rate (Myers et al. 2008; Baudat et al. 2010). However, while *PRDM9* is present in most mammals, it is absent in birds, suggesting different mechanisms of recombination regulation across taxa (Singhal et al. 2015). Furthermore, there are still many unanswered questions, such as why and how the recombination landscapes sometimes differ between sexes, given the observation of higher recombination rates closer to the chromosome ends in males and more uniform recombination landscapes in females (Sardell and Kirkpatrick 2020). Exploring these differences and understanding their underlying mechanisms remain areas of active research.

The initial data of recombination came from direct observations of chiasmata and from segregation of Mendelian traits in model organisms, such as *Drosophila* (Morgan 1910; Haldane 1920; Morton et al. 1976). Subsequently, segregation analysis of molecular markers in large pedigrees became popular for constructing linkage maps and inferring recombination distances in centimorgans (cM) (Robinson 1996; Dumont et al. 2011). Combining physical maps and linkage maps allowed for the inference of local recombination rates along chromosomes (Groenen et al. 2009; Backström et al. 2010; Kawakami et al. 2014; Johnston et al. 2017). The advent of next-generation sequencing (NGS) enabled the screening of dense marker sets in many individuals, facilitating pedigree-free methods to study recombination rates. These methods involve assessing the local level of linkage disequilibrium (LD) and assuming a negative correlation between LD and recombination rate (Singhal et al. 2015; Provost et al. 2022). This has been accompanied by progress in statistics and model inferences of the population-level recombination landscape (McVean and Auton 2007; Chan et al. 2012; Gao et al. 2016; Adrion et al. 2020). Furthermore, dense marker data provided by NGS allows locating individual crossover positions with high precision on chromosomes by

phasing alleles from their segregation pattern in small pedigrees (Smeds et al. 2016), or, as applied most recently, by directly generating haploid data through sperm sequencing (Bell et al. 2020). In birds, high-resolution recombination positioning using NGS-generated single nucleotide polymorphism (SNP) data has so far been applied to a collared flycatcher (*Ficedula albicollis*) three-generation pedigree (Smeds et al. 2016).

In this study, we aim to identify recombination positions at a highly detailed chromosomal scale by analysing genome-wide SNPs segregating in a three-generation pedigree of the great reed warbler (*Acrocephalus arundinaceus*). To achieve this, we sequenced the genomes of the individuals in the pedigree, mapped the reads to the reference genome of the great reed warbler (Sigeman et al. 2021), and called SNPs. Then, we employed the newly developed *RecView* R package (Zhang and Hansson 2023) to analyse the genome-wide SNP data, allowing us to examine the segregation patterns at each SNP in the pedigree and pinpoint recombination positions between genomic regions inherited from different grandparents. Previous studies have indicated significant heterochiasmy in the great reed warbler, with females exhibiting nearly twice the recombination rate compared to males (Hansson et al. 2005; Dawson et al. 2007). However, these earlier studies were limited by the use of few markers covering only small portions of the chromosomes. In contrast, our present study utilises millions of SNPs, which enables us to examine whether recombination events preferentially occur in specific regions of the chromosomes and whether the number and positions of recombination events differ between paternal and maternal chromosomes.

2 Materials and methods

2.1 Generating the SNP dataset

The great reed warbler is a large Acrocephalid warbler and long-distance migrant that spends the winter in sub-Saharan Africa, and returns to breed in reed lakes in Europe and western Asia during the summer (Helbig and Seibold 1999; Lemke et al. 2013; Koleček et al. 2016; Sjöberg et al. 2021). We selected a three-generation pedigree from our long-term study population of great reed warblers at Lake Kvismaren, Sweden (Bensch et al. 1998; Hasselquist 1998; Tarka et al. 2014; Hansson et al. 2018). The pedigree consisted of 12 individuals (**Figure 1**) and included four grandparents (F0 generation), two parents (F1 generation) and six offspring (F2 generation), with the offspring belonging to the 1998 cohort (five males and one female; **Table S1**).

We used a phenol-chloroform protocol to extract genomic DNA from blood (stored in SET buffer) from each of the 12 individuals. Sequencing libraries were created using the TruSeq (Illumina) protocol with 350 bp insert size, and sequenced on a NovaSeq 6000 (Illumina) using a 2×150 bp setup and targeting 50x coverage. Libraries and sequencing were performed by SciLifeLab, Uppsala, Sweden.

The raw sequence reads were trimmed with *trimmomatic* version 0.39 (Bolger et al. 2014), mapped to the reference genome assembly of the great reed warbler (Sigeman et al. 2021) using *bwa mem* version 0.7.17 (Li 2013), and read duplicates were removed with *PicardTools* version 2.27.5 (Broad Institute). Then, variants were called with *freebayes* version 1.3.2 (Garrison and Marth 2012), producing a VCF file. Variants in annotated repeat intervals were removed using *vcftools* version 0.1.16 (Danecek et al. 2011). Only bi-allelic variants were kept, and decomposed for complex and multinucleotide variants, using *vcftools* and *VT decompose_blocksub* version 0.5 (Tan et al. 2015). After indels had been removed

using *vcffilter* from *vcflib* version 2017-04-04 (Garrison et al. 2022), the SNPs were divided into an autosome and a Z-linked dataset. Filtering on quality, strandedness, read placement and genotype coverage (with -f "QUAL > 30 & SAF > 0 & SAR > 0 & RPR > 0 & RPL > 0" and -g "DP > 9" in *vcffilter*) were applied for both datasets. Finally, SNPs with missing data were removed using *vcftools*.

2.2 Chromosome-level assembly and chromosome arms

The genome assembly of the great reed warbler consists of relatively few large scaffolds (Sigeman et al. 2021). Some of the smaller chromosomes are represented by a single scaffold (chromosomes 4A, 13, 14, 19, 20, 23 and 30; Sigeman et al. 2021), and the Z chromosome (which includes a translocated part of chromosome 4A) has previously been assembled to chromosome-level (Ponnikas et al. 2022). The remaining chromosomes are represented by between two and nine scaffolds (Sigeman et al. 2021). To ordered and oriented the scaffolds of the remaining chromosomes, we used synteny analyses to several sources. We used the chromosome-level assemblies of the zebra finch (*Taeniopygia guttata*; bTaeGut1.4.pri, NCBI BioProject ID PRJNA489098) and the great tit (*Parus major*; Parus_major1.1, NCBI BioProject ID PRJNA208335) to assign scaffolds to chromosomes. Next, the scaffolds were ordered and oriented using *de novo* assemblies of two additional great reed warbler individuals (one male and one female; neither being the individual used for the original assembly; constructed with 10X linked read and HiC data) (B. Hansson *et al.*, unpubl. data) and the chromosome-level assembly of another *Acrocephalus* species, the Eurasian reed warbler (*A. scirpaceus*; Sætre et al. 2021). During this process, we detected that the scaffold Contig1 on chromosome 2 was wrongly assembled, and this was corrected (**Table S2**). When the two *de novo* assemblies gave contradictory suggestions about the order or orientation (which could happen for methodological and biological reasons, such as the presence of inversion polymorphisms), we selected the order or orientation that was supported by the

Eurasian reed warbler assembly and/or the recombination analysis in this study (**Table S2**). We did not manage to include some of the micro-chromosomes and chromosome 16 (the latter contains the structurally complicated major histcompatibility complex; Westerdahl et al. 2022). Moreover, one chromosome was deemed too short for reliable analysis of recombination (chromosome 30; 1.3 Mb) and one had several scaffolds with uncertain order and orientation (chromosome 22; see below). Thus, the final number of chromosomes assembled to chromosome-level and included in the present analysis was 29 autosomes and the Z chromosome (**Table S2**), which is similar to that of the great tit and Eurasian reed warbler genome assemblies, but lower compared to the zebra finch where all autosomes are (at least partly) assembled (bTaeGut1.4.pri; NCBI BioProject ID PRJNA489098). We named the chromosomes according to their zebra finch homologs (this study and Sigeman et al. 2021). The total length of the autosomal assembly was 978 Mb, which is similar to the great tit and zebra finch assemblies (1020 and 1056 Mb, respectively).

Autosomes 1, 1A, 2, 3 and 4 are sub-telocentric or sub-metacentric (*i.e.*, have two chromosome arms) in the zebra finch, whereas the remaining autosomes are telocentric (Knief and Forstmeier 2016). For these sub-telocentric or sub-metacentric chromosomes, we estimated the approximate location of the centromere based on low nucleotide diversity among the 12 sequenced individuals (extremely low nucleotide diversity is expected in the centromeric regions; Stump et al. 2005), and its location in the zebra finch (Knief and Forstmeier 2016), and devided them into two arms with the longer arm denoted q and the shorter p (**Table S3**). The Z chromosome is acrocentric in the zebra finch (Knief and Forstmeier 2016), but we did not divide this chromosome in the great reed warbler as there is an exceptionally low nucleotide diversity in a large central part of the great reed warbler Z chromosome (the region between c. 15-70 Mb; total length 87.5 Mb; Ponnikas et al. 2022). However, the Z chromosome has a small pseudoautosomal region (PAR), a region that

recombines with the W chromosome in females. As we have one female offspring in our dataset, which has inherited a W chromosome from its mother, we present data for the PAR (1.1 Mb; where both sexes may recombine) and the non-PAR (86.4 Mb; where only males recombine) of the Z chromosome, separately.

2.3 Localising crossovers using the *RecView* R package

For viewing and locating crossovers (COs), we used *RecView*, an R package that we recently developed specifically for segregation analysis of SNPs in three-generation pedigrees (Zhang and Hansson 2023). *RecView* requires two input files, one providing the order and orientation of the scaffolds of the reference genome, and one providing the genotype data of the individuals. The genotype files for the autosomes and the Z chromosome were generated by extracting genotypes from the VCF files using *vcftools* (command: vcftools --gzvcf [vcf file] --extract-FORMAT-info GT --stdout > [output file]), and converting the data using the *make_012gt()* function in *RecView* (for a description of the input files, see Zhang and Hansson 2023).

In the *RecView* ShinyApp, we seleted the Cumulative Continuity Score (CCS) algorithm with a threshold of 50 (represented with CCS50) to locate the positions of putative COs (for a description of CCS, see Zhang and Hansson 2023). We conducted a manual examination of all CO positions and detected a few artefacts where identical CO positions occurred in more than one offspring and always coincided with scaffold borders. We strongly suspect that this indicates scaffolds that had been wrongly ordered or oriented, and therefore corrected and recalculated the CO positions accordingly (most of these were small and some of them were also supported by the Eurasian reed warbler assembly; corrected order and orientation are given in **Table S2**). However, chromosome 22 had two such problematic scaffolds (contig83 and contig39_split_69700), and since we could not order and orientation these scaffolds reliably, we excluded this chromosome from the analysis (**Table S2**). Thus,

239 our analyses of CO positions included 34 autosomal arms (29 autosomes, five with two arms)
240 and the PAR and non-PAR regions of the Z chromosome (**Table S4**).

241 2.4 Statistical tests

242 For each autosomal arm, we calculated both the sex-average and sex-specific recombination
243 distance (cM) by dividing the number of paternal and maternal COs in the six offspring with
244 the number of analysed meiosis (12 in total; one in each parent for each offspring) and
245 multiplying the value with 100. The recombination distance in cM indicates the probability of
246 observing a recombination event over a specific chromosome region (here, a chromosome
247 arm). Next, the sex-average and sex-specific recombination distances were divided by the
248 size of each autosomal arm to obtain respective recombination rates (cM/Mb). For the Z
249 chromosome, the calculations of recombination distance and rate were the same as for the
250 autosomes, but here we separated between the PAR where both parents may recombine and
251 the rest of the chromosome where only the father may recombine.

252 We tested the difference between sexes in autosomal recombination distance (cM),
253 and in autosomal recombination rate (cM/Mb), with paired t-tests on the autosomal arm-level
254 using the *rstatix* R package (Kassambara 2022). Next, we tested whether CO positions
255 differed between sexes by using both the actual and the proportional positions of COs on the
256 chromosome arms (measured from the telomeric end of the chromosome arms) with a Mann-
257 Whitney U test in the *stats* R package (R Core Team 2022).

258 We used available gene annotations (Sigeman et al. 2021) in *bedtools* (Quinlan and
259 Hall 2010) to explore the overlap between autosomal COs and intergenic, genic, exon, intron,
260 UTR and CDS regions. We focussed on the 6 Mb telomeric ends of the chromosomes
261 because most COs (87%; see Results) were located within these chromosomal regions, and
262 because this 6-Mb region differs from other parts of the chromosomes in, for example, gene
263 density. We tested whether the number of autosomal COs differed between the following

pairs of annotation features: intergenic vs genic regions, exon vs intron, and UTR vs CDS. Here we used chi-squared goodness-of-fit tests with the expected CO-numbers calculated from the total length (in bp) of the intervals of each feature within the 6 Mb regions, using the *rstatix* R package (Kassambara 2022).

We used *tidyverse* R package (Wickham et al. 2019) for data handling, and plotted the results with *ggplot2* (Wickham 2011).

3 Results

We evaluated 408 autosomal arms segregating in the pedigree (34 paternal and 34 maternal chromosome arms for each of the 6 offspring) and located 224 COs, of which 113 were paternal and 111 maternal (**Table S4**). For the Z chromosome, we identified 1 CO in the PAR (of maternal origin) and 6 COs on the remaining part of the Z where only males recombine (Table S4). The estimated precision of the recombination positions was generally high (mean = 557 bp; range 153-8333 bp). Of the 224 autosomal COs, 203 were single CO events on autosomal arms, 18 were double COs (*i.e.*, 9 arms had two COs), and three formed a triple CO event (*i.e.*, one arm had three COs; **Figure 2A**). This means that 213 autosomal arms (203+9+1) had at least 1 CO whereas 195 had no CO (**Figure 2A**). The number of autosomal arms with or without COs did not differ significantly (chi-square test; $\chi^2 = 0.79$, df = 1, p = 0.37). Most cases with more than one CO occurred on larger chromosome arms, and the shortest chromosome arm where this occurred was chromosome 15q (14.9 Mb) for which two COs were detected in two offspring (both originating from the maternal side; **Table S4**). The unique case with three COs on a chromosome arm (in a single offspring) occurred on the long arm (q) of chromosome 4, which is one of the macrochromosomes in songbirds (**Table S4**).

The total number of COs per autosomal arm segregating in the pedigree ranged between 0 and 11 (mean: 6.59) when considering both paternal and maternal COs, between 0

and 7 (mean: 3.32) considering only paternal origins, and between 0 and 6 (mean: 3.26) considering only maternal origins (**Figure 2B-D; Table S4**). This corresponds to sex-average recombination distances for the autosomal arms ranging between 0 and 91.7 cM (mean: 54.9 cM), paternal recombination distances between 0 and 116.7 cM (mean: 55.4 cM), and maternal recombination distances between 0 and 100 cM (mean: 54.4 cM). The recombination distances between paternal and maternal chromosome arms did not differ significantly (paired t-test; t = -0.21, df = 33, p = 0.84). For the Z chromosome, the recombination distance was 8.3 cM for the PAR (sex-average recombination) and 100 cM for the remaining part (paternal recombination).

The sex-average recombination rate for the autosomal arms ranged between 0 and 17.7 cM/Mb (median: 3.06 cM/Mb), whereas the paternal rate varied between 0 and 21.2 cM/Mb (median: 2.93 cM/Mb), and the maternal rate between 0 and 17.7 cM/Mb (median: 2.73 cM/Mb) (**Figure 3A**). There was no significant difference in recombination rate between the sexes (paired t-test; t = -0.16, df = 33, p = 0.88). There was a pronounced non-linear negative association between the recombination rate and the size of the chromosome arms (**Figure 3B**). For the Z chromosome, the recombination rate was 7.58 cM/Mb for the PAR and 1.16 cM/Mb for the remaining part of the chromosome.

The position of the 224 autosomal COs showed strong bias towards the telomeric end of the autosomal arms, and this was true for both paternal and maternal chromosome arms (**Figure 4A**). However, this bias was significantly more pronounced on paternal chromosomes, both when considering the physical distance from the telomeric end (male median position: 1.57 Mb; female median position: 2.10 Mb; Mann-Whitney U test; U = 7732, p = 0.003; **Figure 4B**) and the proportional distance on the chromosome arms (male median position: 9.29%, female median position: 13.14%, Mann-Whitney U test; U = 7365, p = 0.024; **Figure 4C**).

Regarding the distribution of autosomal COs in relation to gene features, 109 COs occurred in intergenic regions and 115 in genic regions, which is not significantly different from an expectation based on the size of these regions (chi-square test; $\chi^2 = 2.77$, df = 1, p = 0.096; **Figure 5A**). Out of the 115 autosomal COs in genic regions, 91 were in introns and 24 in exons, which is significantly different from an expectation based on the size of these regions (chi-square test; $\chi^2 = 3.96$, df = 1, p = 0.047). Note that the data suggest a relatively higher frequency of COs in exons than in introns as exons are much less abundant in the genome than introns. Among the 24 COs in exons, 17 occurred in CDS and 8 in UTRs, which is not significantly different from an expectation based on the size of these regions (chi-square test; $\chi^2 = 1.34$, df = 1, p = 0.25). Regarding the distance to the closest genes, 90% of the autosomal COs were located between -34 kb (upstream) and 47 kb (downstream) to the closest genes (**Figure 5B**).

4 Discussion

Quantifying the recombination landscape and identifying chromosome regions with varying rate of recombination can improve our understanding of the evolutionary impact of gene linkage. Additionally, it can provide insights into the mechanisms underlying the pairing and segregation of homologous chromosomes during meiosis. In this study, we analysed whole-genome sequencing data from a three-generation pedigree of the great reed warbler to precisely locate crossover (CO) events. The high resolution of our analysis enabled us to examine the relationship between COs and various chromosomal features, as well as compare the recombination patterns between paternal and maternal chromosomes.

We observed seven CO events on the Z chromosome, one in the pseudoautosomal region (PAR) of maternal origin, and six in the remaining part where only males recombine. The recombination pattern on the Z chromosome was generally similar to that of similarly sized autosomes, *i.e.*, concentrated towards the chromosome ends. However, since the sex

chromosomes segregate differently in males and females, and since recombination only occurs in the PAR in females, we will not further discuss the few cases of COs on the Z chromosome.

Our analysis focused on 408 autosomal arms segregating in the pedigree (34 arms; 12 meioses per arm among the 6 offspring), and we identified 224 COs. The majority of autosomal arms had either zero or one CO, with only nine cases of two COs and one case of three COs on a single chromosome arm being detected. This implies that 52.2% of the autosomal arms had at least one CO. This finding aligns with two expectations: (i) the probability of a CO product being passed down to the offspring is 50% per chiasma, considering the presence of two sister chromatids with one having a CO, and (ii) the hypothesis of an obligate chiasma requirement, suggesting that at least one chiasma per chromosome arm is necessary for proper segregation of homologous chromosomes (Coop and Przeworski 2007; Stapley et al. 2017). It is worth noting that the terms “crossover” and “chiasma” are sometimes used interchangeably, but that we refer to CO as the genetic recombination event and to chiasma as the cross-shaped interaction between non-sister chromatids of homologous chromosomes during meiotic prophase. The obligate chiasma requirement indicates the necessity to connect homologous chromosome arms, enabling their alignment on the spindle in metaphase I, and thereby facilitating correct segregation (Petronczki et al. 2003). However, there are exceptions to this requirement, most obviously among species exhibiting achiasmy, where chiasmata are absent in one of the sexes (Haldane 1922; Huxley 1928; John et al. 2016). Furthermore, investigations into the obligate chiasma requirement in mammals using cytogenetic and phylogenetic methods identified multiple independent shifts from one chiasma per chromosome arm to one chiasma per chromosome across the phylogenetic tree, extending the hypothesis to a minimum of one CO per chromosome (Dumont 2017). In this study of the great reed warbler pedigree, we detected at

least one CO at all chromosome arms, except for chromosome arm 4p (the short arm; **Table S4**) where we did not detect any CO. This could be due to chance, as zero COs can be expected to occur among 12 meiotic events (one parental and one maternal meiosis for each of the six offspring). Alternatively, it may indicate incomplete assembly of the telomeric end of this chromosome arm, leading to missed CO events, or that the location of the centromere is more telocentric than we estimated from the low nucleotide diversity and its location in the zebra finch. The limited occurrence of chromosome arms with multiple COs in the great reed warbler (ten cases of 213 autosomal arms with at least one CO) supports the notion that CO interference reduces the likelihood of additional COs (Sturtevant 1915; Muller 1916; Otto and Payseur 2019). Notably, recombination interference can be positive, resulting in fewer and/or more spaced COs (Coop and Przeworski 2007) as seems to be the case in great reed warblers, or negative, leading to a higher recombination rate than expected, which is observed in some plants and animals (Auger and Sheridan 2001; Aggarwal et al. 2015).

A study of recombination in humans did not only confirm the obligate chiasma requirement but also emphasised the significance of proper location of chiasmata for accurate segregation of homologous chromosomes during meiosis (Coop and Przeworski 2007). Our analysis revealed an extreme bias of COs towards the sub-telomeric regions of the chromosomes, with approximately 87% of COs occurring within approximately 6 Mb from the chromosome ends. This particular pattern has been observed in various other taxa (Sardell and Kirkpatrick 2020), including in zebra finch and collared flycatcher (Backström et al. 2010; Smeds et al. 2016), indicating a widespread phenomenon. The underlying reason for the bias of COs towards sub-telomeric regions remains an open question. One possibly is that the heterogeneous distribution of COs on chromosomes is regulated by specific DNA sequence structures or motifs. In humans, an overrepresentation of a 13-mer DNA motif has been identified as a factor inducing recombination, with the motif being recognised and

bound by the zinc finger of PRDM9, a histone methyltransferase (Myers et al. 2008). While the *PRDM9* gene is present in many mammals, it is absent in dogs and birds, suggesting that alternative mechanisms exist (Baudat et al. 2010; Paigen and Petkov 2018). Other genes such as *RNF212*, *CPLX1* and *REC8* have been repeatedly implicated in recombination events in mice, humans, cattle and sheep (Reynolds et al. 2013; Kong et al. 2014; Ma et al. 2015; Johnston et al. 2016). A search for DNA motifs associated with recombination in estrildid finches identified a few candidate motifs, but none were found to be causative (Singhal et al. 2015). Likewise, we did not find evidence of overrepresented motifs around the recombination positions that we detected in the great reed warbler (H. Zhang *et al.*, unpublished). Regarding the location of COs in relation to genes, we found that the frequency of COs was similar between intergenic and genic regions. However, within genes, COs occurred more commonly in exons than in introns, suggesting a potential influence of gene structure of recombination events. These patterns differ from those in human and *Drosophila* where recombination rates are generally lower within exons compared to introns and intergenic regions (Kong et al. 2010; Miller et al. 2012).

The number of recombination events was similar between the sexes at both the chromosome and genome level in the great reed warbler, and both sexes exhibited a strong bias towards COs located near the telomeric ends of chromosomes. However, we observed that COs occurred significantly closer to the telomeres on paternal chromosome arms compared to maternal chromosome arms. Previous studies on the great reed warbler, which relied on a limited set of markers but a large multi-generation pedigree, reported approximately twice as high recombination rate in females compared to males (Hansson et al. 2005; Dawson et al. 2007). The discrepancy between these findings and our study likely arises from the fact that the markers used in the former studies were primarily located in the central regions of chromosomes, resulting in an underrepresentation of sub-telomeric CO

414 events, which are biased towards males as observed in the present study. This emphasises the
415 importance of thoroughly screening the entire length of chromosomes to accurately
416 characterise potential sex biases in recombination. In a separate project, we have conducted
417 genotyping using genome-wide distributed restriction site-associated DNA (RAD) markers
418 on a multi-generational pedigree (Ponnikas et al. 2022). Although this dataset had a smaller
419 number of markers (approximately 50k SNPs) compared to the present study (approximately
420 5M SNPs), it included multiple males and females. Preliminary analyses of the autosomal
421 RAD data set confirmed that recombination is biased towards the end of chromosomes in
422 both sexes, and that females have a higher frequency of recombination in the central regions
423 of chromosomes compared to males (S. Ponnikas *et al*., unpublished). Furthermore, male-
424 biased recombination in sub-telomeric regions has been observed in several other taxa
425 including in birds (Backström et al. 2010; Smeds et al. 2016; Sardell and Kirkpatrick 2020),
426 while female-biased recombination around centromeres or centrally on chromosomes has
427 been reported in some cases (Venn et al. 2014; Sutherland et al. 2017; Sardell and
428 Kirkpatrick 2020). Understanding the mechanisms underlying sex differences in the
429 recombination landscape will require considering the combined effects of sex-specific
430 centromeric and telomeric influences, as well as how telomere-guided initiation of
431 recombination clusters COs in sub-telomeric regions in both sexes (Higgins et al. 2012;
432 Haenel et al. 2018; Otto and Payseur 2019).

433 In conclusion, recombination plays a crucial role in evolution by generating new
434 haplotypes that natural selection can act upon. In this study, we utilised whole-genome
435 sequencing data of a three-generation pedigree of the great reed warbler to locate CO
436 positions with high precision and investigate sex-specific patterns of recombination. We
437 found that the overall number of recombination events was similar between the sexes.
438 However, when examining the distribution of CO positions, we discovered a pronounced bias

439 towards the telomeric ends of the chromosomes in both sexes, with a particular strong bias on
440 parental chromosomes. We also found that intra-genic COs were more frequently located
441 within exons than in introns. Elucidating the sex-specific CO landscape in the great reed
442 warbler provides valuable evidence to gain deeper understanding of recombination, a key
443 mechanism in shaping the genetic diversity within populations.

444 Data Availability Statement

445 All sequence data used for this study are accessible under BioProject ID's PRJNA970100.

446 Acknowledgements

447 Sample collection was granted with the appropriate permissions from the Linköpings
448 Djurförsöksetiska nämnd (Dnr 36-11, Dnr 44-14 and ID1633). Sequencing was performed by
449 the SNP&SEQ Technology Platform at Uppsala Genome Center, which is part of National
450 Genomics Infrastructure (NGI) Sweden, and Science for Life Laboratory (SciLifeLab)
451 supported by the Swedish Research Council (and its Council for Research infrastructure,
452 RFI) and the Knut and Alice Wallenberg Foundation. Bioinformatics analyses were
453 performed on computational infrastructure provided by the Swedish National Infrastructure
454 for Computing (SNIC) at Uppsala Multidisciplinary Center for Advanced Computational
455 Science (UPPMAX). Field work was supported by the Kvismare Bird Observatory (report
456 no. xxx).

457 Funding

458 The research was funded by grants from Jörgen Lindström's foundation (to H.Z.), Kungliga
459 Fysiografiska Sällskapet (to H.Z.), the European Research Council (ERC) under the
460 European Union's Horizon 2020 research and innovation program (Advanced grant 742646

461 to D.H.) and the Swedish Research Council (grants no. 2016-04391 and 2020-03976 to D.H.,
462 and 2016-00689 and 2022-04996 to B.H.).

463 Author contributions

464 H.Z., D.H. and B.H. designed and planned the study. H.Z. performed the laboratory work of
465 preparing genomic DNA. H.Z. performed the bioinformatic analyses with input from M.L
466 and B.H. H.Z. and B.H. wrote the manuscript with input from M.L., S.P., and D.H. All
467 authors approved the final version of the manuscript.

468 Conflict of Interest

469 The authors have no conflict of interest to declare.

470 Reference

471 Adrion JR, Galloway JG, Kern AD. 2020. Predicting the landscape of recombination using deep learning. *Mol.*
472 *Biol. Evol.* 37:1790–1808.
473 Aggarwal DD, Rashkovetsky E, Michalak P, Cohen I, Ronin Y, Zhou D, Haddad GG, Korol AB. 2015.
474 Experimental evolution of recombination and crossover interference in Drosophila caused by directional
475 selection for stress-related traits. *BMC Biol.* 13:101.
476 Arbeithuber B, Betancourt AJ, Ebner T, Tiemann-Boege I. 2015. Crossovers are associated with mutation and
477 biased gene conversion at recombination hotspots. *Proc. Natl. Acad. Sci.* 112:2109–2114.
478 Auger DL, Sheridan WF. 2001. Negative Crossover Interference in Maize Translocation Heterozygotes.
479 *Genetics* 159:1717–1726.
480 Bachtrog D. 2013. Y-chromosome evolution: emerging insights into processes of Y-chromosome degeneration.
481 *Nat. Rev. Genet.* 14:113–124.
482 Backström N, Forstmeier W, Schielzeth H, Mellenius H, Nam K, Bolund E, Webster MT, Öst T, Schneider M,
483 Kempenaers B, et al. 2010. The recombination landscape of the zebra finch *Taeniopygia guttata* genome.
484 *Genome Res.* 20:485–495.
485 Baudat F, Buard J, Grey C, Fledel-Alon A, Ober C, Przeworski M, Coop G, De Massy B. 2010. PRDM9 Is a
486 Major Determinant of Meiotic Recombination Hotspots in Humans and Mice. *Science* 327:836–840.
487 Bell AD, Mello CJ, Nemesh J, Brumbaugh SA, Wysoker A, McCarroll SA. 2020. Insights into variation in
488 meiosis from 31,228 human sperm genomes. *Nature* 583:259–264.
489 Bensch S, Hasselquist D, Nielsen B, Hansson B. 1998. Higher Fitness for Philopatric than for Immigrant Males
490 in a Semi-Isolated Population of Great Reed Warblers. *Evolution* 52:877–883.
491 Bergero R, Gardner J, Bader B, Yong L, Charlesworth D. 2019. Exaggerated heterochiasmy in a fish with sex-
492 linked male coloration polymorphisms. *Proc. Natl. Acad. Sci.* 116:6924–6931.
493 Berset-Brändli L, Jaquiéry J, Broquet T, Ulrich Y, Perrin N. 2008. Extreme heterochiasmy and nascent sex
494 chromosomes in European tree frogs. *Proc. R. Soc. B Biol. Sci.* 275:1577–1585.
495 Bolger AM, Lohse M, Usadel B. 2014. Trimmomatic: a flexible trimmer for Illumina sequence data.
496 *Bioinformatics* 30:2114–2120.
497 Broad Institute. Picard Tools. Available from: https://broadinstitute.github.io/picard/
498 Broman KW, Murray JC, Sheffield VC, White RL, Weber JL. 1998. Comprehensive Human Genetic Maps:
499 Individual and Sex-Specific Variation in Recombination. *Am. J. Hum. Genet.* 63:861–869.

Burt A, Bell G, Harvey PH. 1991. Sex differences in recombination. *J. Evol. Biol.* 4:259–277.

Chan AH, Jenkins PA, Song YS. 2012. Genome-Wide Fine-Scale Recombination Rate Variation in *Drosophila melanogaster*.McVean G, editor. *PLoS Genet.* 8:e1003090.

Charlesworth Brian, Charlesworth D. 2000. The degeneration of Y chromosomes.Charlesworth B., Harvey PH, editors. *Philos. Trans. R. Soc. Lond. B. Biol. Sci.* 355:1563–1572.

Coop G, Przeworski M. 2007. An evolutionary view of human recombination. *Nat. Rev. Genet.* 8:23–34.

Danecek P, Auton A, Abecasis G, Albers CA, Banks E, DePristo MA, Handsaker RE, Lunter G, Marth GT, Sherry ST, et al. 2011. The variant call format and VCFtools. *Bioinformatics* 27:2156–2158.

Dawson DA, Akesson M, Burke T, Pemberton JM, Slate J, Hansson B. 2007. Gene Order and Recombination Rate in Homologous Chromosome Regions of the Chicken and a Passerine Bird. *Mol. Biol. Evol.* 24:1537–1552.

Dumont BL. 2017. Variation and Evolution of the Meiotic Requirement for Crossing Over in Mammals. *Genetics* 205:155–168.

Dumont BL, Payseur BA. 2008. Evolution of the genomic rate of recombination in mammals. *Evolution* 62:276–294.

Dumont BL, White MA, Steffy B, Wiltshire T, Payseur BA. 2011. Extensive recombination rate variation in the house mouse species complex inferred from genetic linkage maps. *Genome Res.* 21:114–125.

Ellermeier C, Higuchi EC, Phadnis N, Holm L, Geelhood JL, Thon G, Smith GR. 2010. RNAi and heterochromatin repress centromeric meiotic recombination. *Proc. Natl. Acad. Sci.* 107:8701–8705.

Felsenstein J. 1974. The evolutionary advantage of recombination. *Genetics* 78:737–756.

Filatov DA, Gerrard DT. 2003. High mutation rates in human and ape pseudoautosomal genes. *Gene* 317:67–77.

Gao F, Ming C, Hu W, Li H. 2016. New software for the fast estimation of population recombination rates (FastEPRR) in the genomic era. *G3 Genes Genomes Genet.* 6:1563–1571.

Garrison E, Kronenberg ZN, Dawson ET, Pedersen BS, Prins P. 2022. A spectrum of free software tools for processing the VCF variant call format: vcflib, bio-vcf, cyvcf2, hts-nim and slivar. *PLOS Comput. Biol.* 18:e1009123.

Garrison E, Marth G. 2012. Haplotype-based variant detection from short-read sequencing. *ArXiv Prepr.*:1207.3907.

Groenen MAM, Wahlberg P, Foglio M, Cheng HH, Megens H-J, Crooijmans RPMA, Besnier F, Lathrop M, Muir WM, Wong GK-S, et al. 2009. A high-density SNP-based linkage map of the chicken genome reveals sequence features correlated with recombination rate. *Genome Res.* 19:510–519.

Haenel Q, Laurentino TG, Roesti M, Berner D. 2018. Meta-analysis of chromosome-scale crossover rate variation in eukaryotes and its significance to evolutionary genomics. *Mol. Ecol.* 27:2477–2497.

Haldane J. 1920. Note on a case of linkage in *Paratettix*. *J. Genet.* 10:47–51.

Haldane JB. 1922. Sex ratio and unisexual sterility in hybrid animals. *J. Genet.* 12:101–109.

Halldorsson BV, Palsson G, Stefansson OA, Jonsson H, Hardarson MT, Eggertsson HP, Gunnarsson B, Oddsson A, Halldorsson GH, Zink F, et al. 2019. Characterizing mutagenic effects of recombination through a sequence-level genetic map. *Science* 363:eaau1043.

Hansson B, Åkesson M, Slate J, Pemberton JM. 2005. Linkage mapping reveals sex-dimorphic map distances in a passerine bird. *Proc. R. Soc. B Biol. Sci.* 272:2289–2298.

Hansson B, Sigeman H, Stervander M, Tarka M, Ponnikas S, Strandh M, Westerdahl H, Hasselquist D. 2018. Contrasting results from GWAS and QTL mapping on wing length in great reed warblers. *Mol. Ecol. Resour.* 18:867–876.

Hasselquist D. 1998. Polygyny in great reed warblers: a long-term study of factors contributing to male fitness. *Ecology* 79:2376–2390.

Helbig AJ, Seibold I. 1999. Molecular Phylogeny of Palearctic–African *Acrocephalus* and *Hippolais* Warblers (Aves: Sylviidae). *Mol. Phylogenet. Evol.* 11:246–260.

Hellmann I, Ebersberger I, Ptak SE, Pääbo S, Przeworski M. 2003. A Neutral Explanation for the Correlation of Diversity with Recombination Rates in Humans. *Am. J. Hum. Genet.* 72:1527–1535.

Higgins JD, Perry RM, Barakate A, Ramsay L, Waugh R, Halpin C, Armstrong SJ, Franklin FCH. 2012. Spatiotemporal Asymmetry of the Meiotic Program Underlies the Predominantly Distal Distribution of Meiotic Crossovers in Barley. *Plant Cell* 24:4096–4109.

Huang S-W, Friedman R, Yu N, Yu A, Li W-H. 2005. How Strong Is the Mutagenicity of Recombination in Mammals? *Mol. Biol. Evol.* 22:426–431.

Huxley J. 1928. Sexual difference of linkage in *Gammarus chevreuxi*. *J. Genet.* 20:145–156.

John A, Vinayan K, Varghese J. 2016. Achiasmy: Male Fruit Flies Are Not Ready to Mix. *Front. Cell Dev. Biol.* [Internet] 4. Available from: http://journal.frontiersin.org/Article/10.3389/fcell.2016.00075/abstract

Johnston SE, Bérénos C, Slate J, Pemberton JM. 2016. Conserved Genetic Architecture Underlying Individual Recombination Rate Variation in a Wild Population of Soay Sheep (*Ovis aries*). *Genetics* 203:583–598.

Johnston SE, Huisman J, Ellis PA, Pemberton JM. 2017. A High-Density Linkage Map Reveals Sexual Dimorphism in Recombination Landscapes in Red Deer (*Cervus elaphus*). *G3 GenesGenomesGenetics* 7:2859–2870.

Kassambara A. 2022. rstatix: Pipe-friendly framework for basic statistical tests. R package version 0.7.1. Available from: https://CRAN.R-project.org/package=rstatix

Kawakami T, Smeds L, Backström N, Husby A, Qvarnström A, Mugal CF, Olason P, Ellegren H. 2014. A high-density linkage map enables a second-generation collared flycatcher genome assembly and reveals the patterns of avian recombination rate variation and chromosomal evolution. *Mol. Ecol.* 23:4035–4058.

Knief U, Forstmeier W. 2016. Mapping centromeres of microchromosomes in the zebra finch (*Taeniopygia guttata*) using half-tetrad analysis. *Chromosoma* 125:757–768.

Kohl KP, Singh ND. 2018. Experimental evolution across different thermal regimes yields genetic divergence in recombination fraction but no divergence in temperature associated plastic recombination. *Evolution* 72:989–999.

Koleček J, Procházka P, El-Arabany N, Tarka M, Ilieva M, Hahn S, Honza M, De La Puente J, Bermejo A, Gürsoy A, et al. 2016. Cross-continental migratory connectivity and spatiotemporal migratory patterns in the great reed warbler. *J. Avian Biol.* 47:756–767.

Kong A, Barnard J, Gudbjartsson DF, Thorleifsson G, Jonsdottir G, Sigurdardottir S, Richardsson B, Jonsdottir J, Thorgeirsson T, Frigge ML, et al. 2004. Recombination rate and reproductive success in humans. *Nat. Genet.* 36:1203–1206.

Kong A, Thorleifsson G, Frigge ML, Masson G, Gudbjartsson DF, Villemoes R, Magnusdottir E, Olafsdottir SB, Thorsteinsdottir U, Stefansson K. 2014. Common and low-frequency variants associated with genome-wide recombination rate. *Nat. Genet.* 46:11–16.

Kong A, Thorleifsson G, Gudbjartsson DF, Masson G, Sigurdsson A, Jonasdottir Aslaug, Walters GB, Jonasdottir Adalbjorg, Gylfason A, Kristinsson KT, et al. 2010. Fine-scale recombination rate differences between sexes, populations and individuals. *Nature* 467:1099–1103.

Lemke HW, Tarka M, Klaassen RHG, Åkesson M, Bensch S, Hasselquist D, Hansson B. 2013. Annual Cycle and Migration Strategies of a Trans-Saharan Migratory Songbird: A Geolocator Study in the Great Reed Warbler.Saino N, editor. *PLoS ONE* 8:e79209.

Li H. 2013. Aligning sequence reads, clone sequences and assembly contigs with BWA-MEM. *ArXiv Prepr.*:1303.3997.

Limborg MT, McKinney GJ, Seeb LW, Seeb JE. 2016. Recombination patterns reveal information about centromere location on linkage maps. *Mol. Ecol. Resour.* 16:655–661.

Ma L, O'Connell JR, VanRaden PM, Shen B, Padhi A, Sun C, Bickhart DM, Cole JB, Null DJ, Liu GE, et al. 2015. Cattle Sex-Specific Recombination and Genetic Control from a Large Pedigree Analysis.Auton AJ, editor. *PLOS Genet.* 11:e1005387.

Maddox JF, Davies KP, Crawford AM, Hulme DJ, Vaiman D, Cribiu EP, Freking BA, Beh KJ, Cockett NE, Kang N, et al. 2001. An enhanced linkage map of the sheep genome comprising more than 1000 loci. *Genome Res.* 11:1275–1289.

Malinovskaya LP, Tishakova K, Shnaider EP, Borodin PM, Torgasheva AA. 2020. Heterochiasmy and Sexual Dimorphism: The Case of the Barn Swallow (Hirundo rustica, Hirundinidae, Aves). *Genes* 11:1119.

McVean G, Auton A. 2007. LDhat 2.1: a package for the population genetic analysis of recombination. *Dep. Stat. Oxf. OX1 3TG UK*.

Melamed-Bessudo C, Levy AA. 2012. Deficiency in DNA methylation increases meiotic crossover rates in euchromatic but not in heterochromatic regions in *Arabidopsis*. *Proc. Natl. Acad. Sci.* [Internet] 109. Available from: https://pnas.org/doi/full/10.1073/pnas.1120742109

Miller DE, Takeo S, Nandanan K, Paulson A, Gogol MM, Noll AC, Perera AG, Walton KN, Gilliland WD, Li H, et al. 2012. A whole-chromosome analysis of meiotic recombination in Drosophila melanogaster. *G3 Genes Genomes Genet.* 2:249–260.

Morgan TH. 1910. Sex limited inheritance in *Drosophila*. *Science* 32:120–122.

Morton N, Rao D, Yee S. 1976. An inferred chiasma map of *Drosophila melanogaster*. *Heredity* 37:405–411.

Mugal CF, Weber CC, Ellegren H. 2015. GC-biased gene conversion links the recombination landscape and demography to genomic base composition: GC-biased gene conversion drives genomic base composition across a wide range of species. *BioEssays* 37:1317–1326.

Muller HJ. 1916. The mechanism of crossing-over. *Am. Nat.* 50:193–221.

Myers S, Freeman C, Auton A, Donnelly P, McVean G. 2008. A common sequence motif associated with recombination hot spots and genome instability in humans. *Nat. Genet.* 40:1124–1129.

Otto SP. 2021. Selective Interference and the Evolution of Sex. *J. Hered.* 112:9–18.

Otto SP, Payseur BA. 2019. Crossover Interference: Shedding Light on the Evolution of Recombination. *Annu. Rev. Genet.* 53:19–44.

Paigen K, Petkov PM. 2018. PRDM9 and Its Role in Genetic Recombination. *Trends Genet.* 34:291–300.

Peñalba JV, Wolf JBW. 2020. From molecules to populations: appreciating and estimating recombination rate variation. *Nat. Rev. Genet.* 21:476–492.

Petronczki M, Siomos MF, Nasmyth K. 2003. Un menage a quatre: the molecular biology of chromosome segregation in meiosis. *Cell* 112:423–440.

Ponnikas S, Sigeman H, Lundberg M, Hansson B. 2022. Extreme variation in recombination rate and genetic diversity along the Sylvioidea neo-sex chromosome. *Mol. Ecol.* 31:3566–3583.

Provost K, Shue SY, Forcellati M, Smith BT. 2022. The genomic landscapes of desert birds form over multiple time scales. *Mol. Biol. Evol.* 39:msac200.

Quinlan AR, Hall IM. 2010. BEDTools: a flexible suite of utilities for comparing genomic features. *Bioinformatics* 26:841–842.

R Core Team. 2022. R: A language and environment for statistical computing. *R Found. Stat. Comput. Vienna Austria* [Internet]. Available from: https://www.R-project.org/

Reynolds A, Qiao H, Yang Y, Chen JK, Jackson N, Biswas K, Holloway JK, Baudat F, De Massy B, Wang J, et al. 2013. RNF212 is a dosage-sensitive regulator of crossing-over during mammalian meiosis. *Nat. Genet.* 45:269–278.

Ritz KR, Noor MA, Singh ND. 2017. Variation in recombination rate: adaptive or not? *Trends Genet.* 33:364–374.

Robinson WP. 1996. The Extent, Mechanism, and Consequences of Genetic Variation, for Recombination Rate. *Am J Hum Genet*.

Sætre CLC, Eroukhmanoff F, Rönkä K, Kluen E, Thorogood R, Torrance J, Tracey A, Chow W, Pelan S, Howe K, et al. 2021. A Chromosome-Level Genome Assembly of the Reed Warbler (*Acrocephalus scirpaceus*).Fraser B, editor. *Genome Biol. Evol.* 13:evab212.

Sardell JM, Kirkpatrick M. 2020. Sex Differences in the Recombination Landscape. *Am. Nat.* 195:361–379.

Sigeman H, Strandh M, Proux-Wéra E, Kutschera VE, Ponnikas S, Zhang H, Lundberg M, Soler L, Bunikis I, Tarka M, et al. 2021. Avian Neo-Sex Chromosomes Reveal Dynamics of Recombination Suppression and W Degeneration.Wilson M, editor. *Mol. Biol. Evol.* 38:5275–5291.

Singhal S, Leffler EM, Sannareddy K, Turner I, Venn O, Hooper DM, Strand AI, Li Q, Raney B, Balakrishnan CN. 2015. Stable recombination hotspots in birds. *Science* 350:928–932.

Sjöberg S, Malmiga G, Nord A, Andersson A, Bäckman J, Tarka M, Willemoes M, Thorup K, Hansson B, Alerstam T, et al. 2021. Extreme altitudes during diurnal flights in a nocturnal songbird migrant. *Science* 372:646–648.

Smeds L, Mugal CF, Qvarnström A, Ellegren H. 2016. High-Resolution Mapping of Crossover and Non-crossover Recombination Events by Whole-Genome Re-sequencing of an Avian Pedigree.Henderson I, editor. *PLOS Genet.* 12:e1006044.

Stapley J, Feulner PGD, Johnston SE, Santure AW, Smadja CM. 2017. Variation in recombination frequency and distribution across eukaryotes: patterns and processes. *Philos. Trans. R. Soc. B Biol. Sci.* 372:20160455.

Stump AD, Fitzpatrick MC, Lobo NF, Traoré S, Sagnon N, Costantini C, Collins FH, Besansky NJ. 2005. Centromere-proximal differentiation and speciation in *Anopheles gambiae*. *Proc. Natl. Acad. Sci.* 102:15930–15935.

Sturtevant AH. 1915. The behavior of the chromosomes as studied through linkage. *Z. Für Indukt. Abstamm.-Vererbungslehre* 13:234–287.

Sutherland BJ, Rico C, Audet C, Bernatchez L. 2017. Sex chromosome evolution, heterochiasmy, and physiological QTL in the salmonid brook charr Salvelinus fontinalis. *G3 Genes Genomes Genet.* 7:2749–2762.

Tan A, Abecasis GR, Kang HM. 2015. Unified representation of genetic variants. *Bioinformatics* 31:2202–2204.

Tarka M, Åkesson M, Hasselquist D, Hansson B. 2014. Intralocus Sexual Conflict over Wing Length in a Wild Migratory Bird. *Am. Nat.* 183:62–73.

Venn O, Turner I, Mathieson I, De Groot N, Bontrop R, McVean G. 2014. Strong male bias drives germline mutation in chimpanzees. *Science* 344:1272–1275.

Vincenten N, Kuhl L-M, Lam I, Oke A, Kerr AR, Hochwagen A, Fung J, Keeney S, Vader G, Marston AL. 2015. The kinetochore prevents centromere-proximal crossover recombination during meiosis. *eLife* 4:e10850.

Wellenreuther M, Sánchez-Guillén RA, Cordero-Rivera A, Svensson EI, Hansson B. 2013. Male-biased recombination in odonates: insights from a linkage map of the damselfly *Ischnura elegans*. *J. Genet.* 92:115–119.

Westerdahl H, Mellinger S, Sigeman H, Kutschera VE, Proux-Wéra E, Lundberg M, Weissensteiner M, Churcher A, Bunikis I, Hansson B, et al. 2022. The genomic architecture of the passerine MHC region: High repeat content and contrasting evolutionary histories of single copy and tandemly duplicated MHC genes. *Mol. Ecol. Resour.* 22:2379–2395.

Wickham H. 2011. ggplot2. *Wiley Interdiscip. Rev. Comput. Stat.* 3:180–185.

Wickham H, Averick M, Bryan J, Chang W, McGowan LD, François R, Grolemund G, Hayes A, Henry L, Hester J, et al. 2019. Welcome to the Tidyverse. *J. Open Source Softw.* 4:1686.

Wijnker E, Velikkakam James G, Ding J, Becker F, Klasen JR, Rawat V, Rowan BA, De Jong DF, De Snoo CB, Zapata L, et al. 2013. The genomic landscape of meiotic crossovers and gene conversions in *Arabidopsis thaliana*. *eLife* 2:e01426.

Zhang H, Hansson B. 2023. RecView: an interactive R application for locating recombination positions using pedigree data. *BMC Genomics* 24:1–10.

Figures

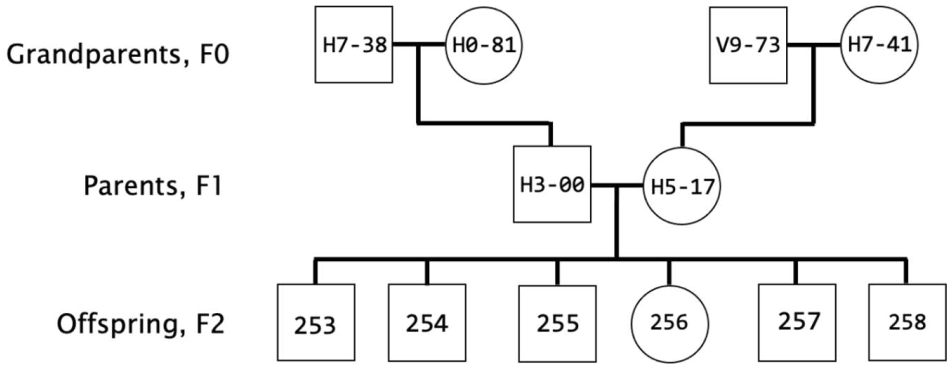

Figure 1. The three-generation great reed warbler pedigree analysed in the present study. Project-specific individual codes are given. Squares show males, circles females.

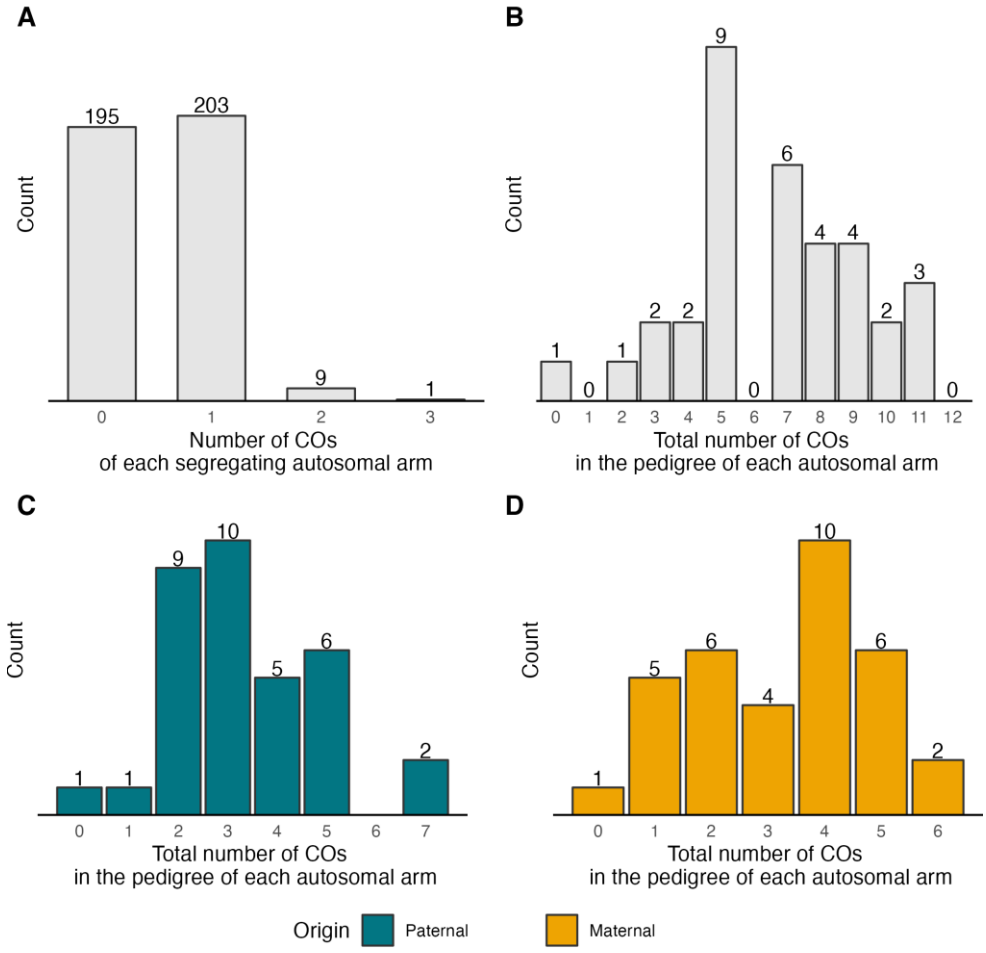

Figure 2. (A) The distribution of crossovers (COs) of each segregating autosomal arm. The total number of segregating autosomal arms evaluated was 408 (34 paternal and 34 maternal autosomal arms for each of the six offspring). (B-D) The distribution of the total number of COs in the pedigree of each autosomal arm (n = 34) considering COs of (B) both paternal and maternal origin, (C) only paternal origin, and (D) only maternal origin.

704

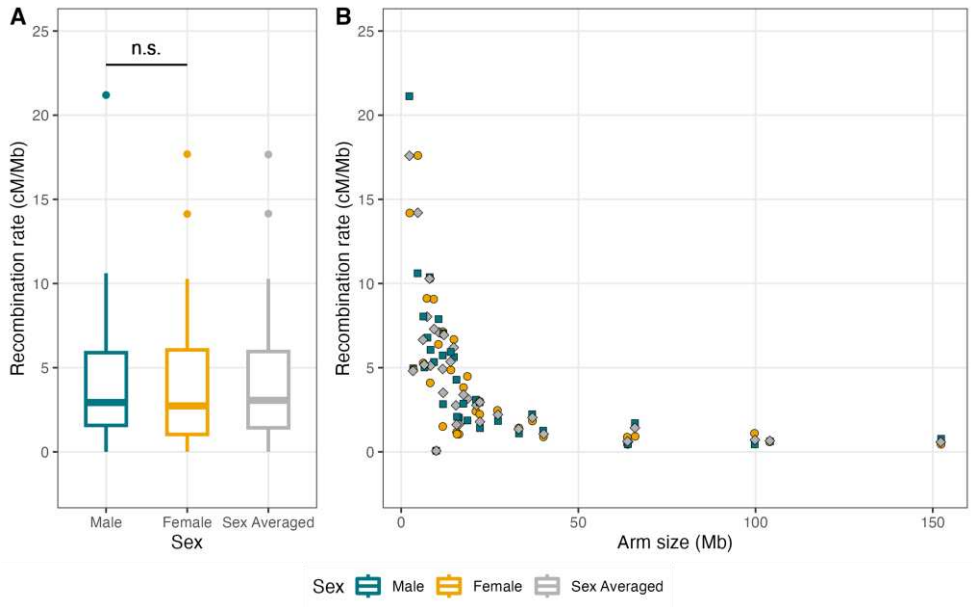

705

706 **Figure 3**. (A) The distribution of male, female and sex-averaged recombination rates on
707 autosomal arms. (B) The association between the male (green rectangles), female (yellow
708 circles) and sex-averaged (grey diamonds) recombination rates and the size of autosomal
709 arms.

710

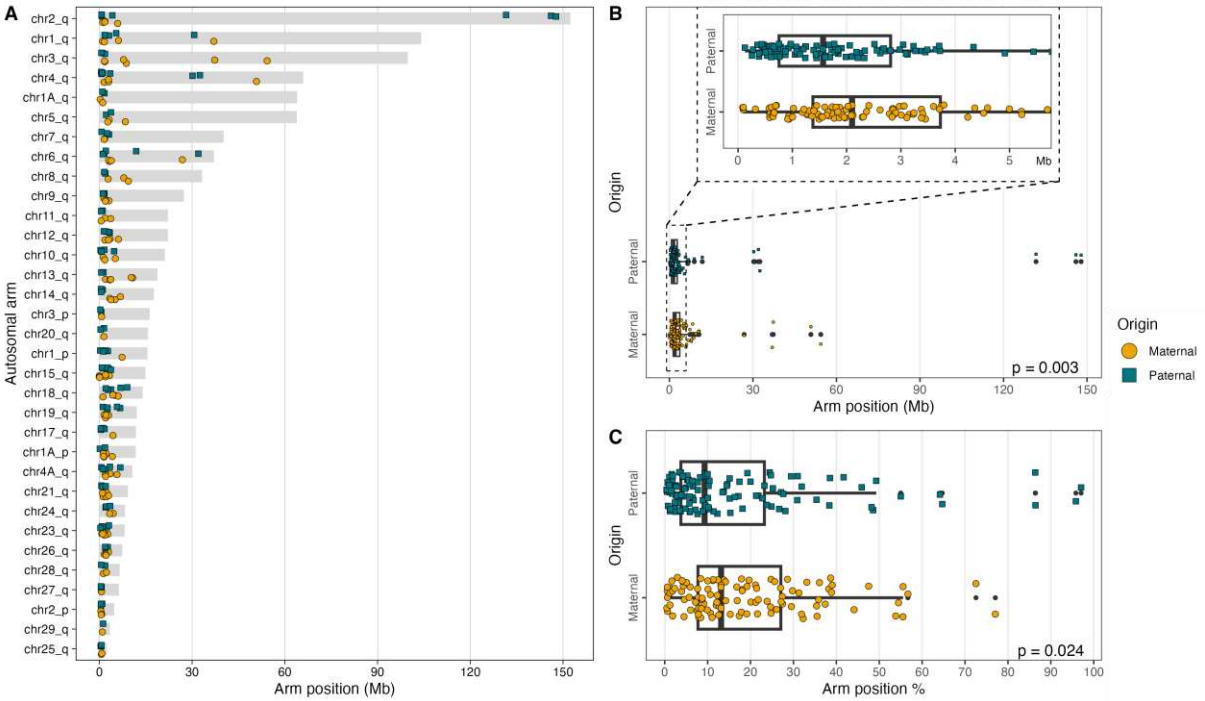

Figure 4. The bias of COs towards the telomeric ends of chromosomes. (A) The location of CO positions of paternal and maternal origins on each chromosome arm. (B) The physical distance of CO positions from the telomeric end of autosomal arms. (C) The proportional distance of CO positions from the telomeric end of autosomal arms. Grey bars (A) indicate the sizes of the autosomal arms. The colouration and shape of points (A-C) indicate paternal (green squares) and maternal (yellow circles) CO events.

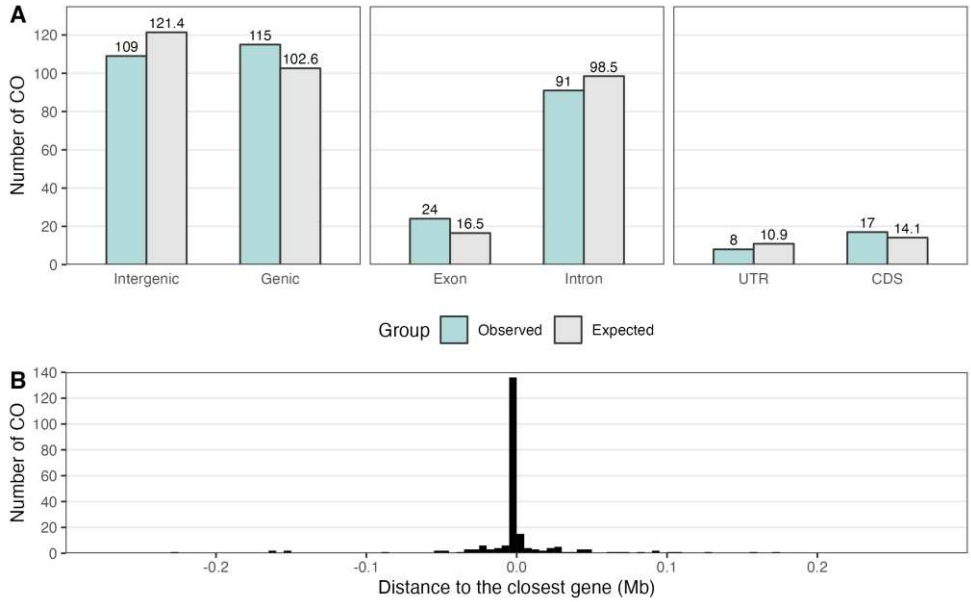

719

720 **Figure 5.** The relationship between autosomal CO events and gene features. (A) Number of
721 COs in intergenic and genic regions, in exons and introns, and in UTR and CDS (green bars).
722 Aslo given are the expected numbers based on the size of these gene features within 6 Mb of
723 the end of the chromosome arms (grey bars). (B) The distribution of the distance to the
724 closest gene for autosomal CO events.